Time History Earthquake Response Analysis Using Causal Hysteretic Damping Model

Naohiro Nakamura[1]

[1] *Dr. Eng., Chief Researcher, R&D Institute, Takenaka Corporation, Chiba Pref,. Japan*
E-mail: nakamura.naohiro@takenaka.co.jp

ABSTRACT :

A number of experiments indicate that the internal damping corresponding to the energy dissipation of many materials is essentially frequency independent. Accordingly, an analysis model that can express such characteristics (called a hysteretic damping model) in the time domain is needed. Although a great number of investigations into this subject have been carried out, there are few practical methods. In this paper, a simple and practical hysteretic damping model that can be applied to time history response analyses is proposed. First, a unit imaginary function that is a principle factor of the hysteretic damping model is considered, and a causal function approximating to this is selected. This function is transformed to the impulse response in the time domain. The proposed causal hysteretic damping model is made using 2*h* times the impulse response, where *h* is the damping ratio. Next, the Biot model is described and the characteristics of the impedance and the impulse response of the model are compared with those of the proposed model. Then, in order to confirm the applicability and the efficiency of the proposed model to time history response analyses, earthquake response analyses of example models are carried out.

KEYWORDS: hysteretic damping, causality, time history analysis, the Biot model

1. INTRODUCTION

It is well known that the hysteretic dissipation energy with regard to the internal damping of many materials is essentially frequency independent (e.g. Chopra(2000)). A damping model indicating such characteristics is called a hysteretic damping model (either a complex damping model or a structural damping model).
In cases where not only the effects of the first natural mode of a structure, but also those of higher natural modes cannot be ignored in the response estimation of the structure, or in the case of the natural frequency of the structure varying due to the nonlinear behavior of the structure, the use of the aforementioned damping model is particularly required.
In analyses carried out in a frequency domain, a hysteretic damping model that can be expressed using a complex spring with constant coefficient for ω in both real and imaginary parts is often used. However, in order to take into account the effects of the nonlinear behavior during a severe earthquake, it is necessary to carry out tine history response analyses.
As damping models in the time history analysis, the Kelvin-Voigt model, the Rayleigh model and the strain energy proportioned model (Dobry et all. 1971) are often applied. The Kelvin-Voigt model is simple and widely used, but the damping ratio is proportional to frequency. The damping ratio of the Rayleigh model is frequency independent to some degree, but it becomes large in the lower and the higher frequency range. The damping ratio of the strain energy proportioned model is almost frequency independent in the wide frequency range. However, this model is not widely used because the calculation is not simple, e.g. an eigenvalue analysis up to high order is essential and the damping matrix becomes a full matrix. So there are problems in accuracy and applicability in these methods.
It is well known that a precise transform of the hysteretic damping model to the time domain is impossible due to the fact that it is noncausal and does not satisfy the Kramers-Kroning relation (e.g. Inaudi and Kelly, 1995). A number of studies on a hysteretic damping model that satisfies the causality have been carried out.
For example, Inaudi and Kelly (1995) presented a precise hysteretic damping model in the tine domain based on the Hilbert transform and proposed a method for applying it to time history analyses by conducting convergent calculations. Makris (1997) proposed a causal model that can be placed at the limit of Biot's visco-

elastic model (Biot, 1958) and showed that this model is closer to the ideal hysteretic damping than the Biot model. Afterwards, Makris and Zhang (2000) compared the model with the Biot model minutely and showed that the Biot model is more practical and reliable than the model for actual time-domain analyses. They also approximated the Biot model simply by the Prony series and showed the efficiency of the model by applying it to the response analyses of a soil structure. Therefore, the Biot model has been regarded as one of the models which most closely approximate the hysteretic damping among causal models. However, the model has not been widely used yet in practical time history analyses and more effective damping models are needed.

The author proposed some methods for the transform of the frequency dependent complex stiffness to the time domain (Nakamura, 2006a, 2006b). The frequency independent hysteretic damping can be considered to be the damping in a special case for the frequency dependent complex stiffness.

In this paper, a simple and practical hysteretic damping model that can be applied to time history response analyses is proposed on the basis of the previous study.

First, the concept of the proposed damping model is explained and the characteristics of the model both in the time domain and in the frequency domain are investigated.

Next, the Biot model formulated base on Makris and Zhang (2000) is described and the characteristics of the impedance and the impulse response of the model are compared with those of the proposed model.

Moreover, with a view to estimating the applicability and the efficiency of the proposed model to time history response analyses in comparison with the energy proportional damping model and the Biot model, earthquake response analyses of both a 4 node model and a layered soil model are carried out.

2. MODELING METHOD

2.1 Concept of Proposed Model

The complex stiffness including the hysteretic damping is given by Eq. 2.1. Where K_0: Stiffness, h: Damping ratio, i: Imaginary unit.

$$S(\omega) = K_0(1 + 2h \cdot i \cdot \mathrm{sgn}(\omega)) \tag{2.1}$$

Using $Z(\omega)$ in Eq.2.2, Eq. 2.1 is replaced by Eq. 2.4.

$$Z(\omega) = Z_R(\omega) + Z_I(\omega) \cdot i \tag{2.2}$$

Where

$$Z_R(\omega) = 0, \quad Z_I(\omega) = 1 \ (\omega > 0), \ = 0 \ (\omega = 0), \ = -1 \ (\omega < 0) \tag{2.3}$$

$$S(\omega) = K_0 \cdot (1 + 2h \cdot Z(\omega)) \tag{2.4}$$

It is impossible to transform $Z(\omega)$ (hereafter referred to as unit imaginary function) accurately to the time domain. Therefore, in this paper Eq. 2.5 is formulated using the causalized unit imaginary function $Z'(\omega)$ (hereafter referred to as causal unit imaginary function) in order to transform it to the time domain by relaxing the conditions as indicated below.

$$S'(\omega) = K_0(1 + 2h \cdot Z'(\omega)) \tag{2.5}$$

1) Consideration of focused frequency range

In many earthquake response analyses of structures, the frequency subjected to investigations is 10Hz or less. The frequency for rigid structures such as nuclear power plant facilities is 20Hz or less. A frequency of over 20Hz hardly contributes to the structural response in most cases.

Therefore, it is thought that Eq. 2.3 is to be formed only in a certain fixed frequency range ($-\omega_m < \omega < \omega_m$ hereafter referred to as focused frequency range). It is also important that the value $Z(\omega)$ on the outside of the range must not exert a negative influence upon the response value, as described later.

2) Reevaluation of real part

In order that the complex stiffness is causal, both the real part and the imaginary part need to satisfy the Kramers-Kroning relation. In this paper, the real part is to be reevaluated from the Hilbert transform of the imaginary part. Consequently, the real part ($Z_R(\omega)$) becomes the frequency dependent value (hereafter referred to as $Z'_R(\omega)$) from 0.

2.2 Modeling of Imaginary Part

The imaginary part of the proposed model (hereafter referred to as $Z'_I(\omega)$) is shown as the sum of the regular component $Z'_{Ir}(\omega)$ and the singular component $Z'_{Is}(\omega)$ in Eqs 2.6, 2.7 and Figure 1.

The figure shows the values in the range of $\omega>0$ with the skew-symmetry in the range of $\omega<0$. The regular component $Z'_{Ir}(\omega)$ is set as a function repeating at every ω_m. In the outside of the focused frequency range, the regular component is a function that increases by steps along with the singular component as shown in Figure 2. Namely, with a rise in ω, the total imaginary part increases and becomes rigid at $\omega \to \infty$. Therefore, it is thought that the effect of the matter outside of the focused frequency range upon the response is slight.

$$Z'_I(\omega) = Z'_{Ir}(\omega) + Z'_{Is}(\omega) \tag{2.6}$$

$$Z'_{Ir}(\omega) = (2n-1) - \frac{2\omega}{\omega_m}, \quad Z'_{Is}(\omega) = \frac{2\omega}{\omega_m} \tag{2.7}$$

Where $n=1\ (0 \le \omega < \omega_m)$, $n=2\ (\omega_m \le \omega < 2\omega_m)$, $n=3\ (2\omega_m \le \omega < 3\omega_m), \cdots$

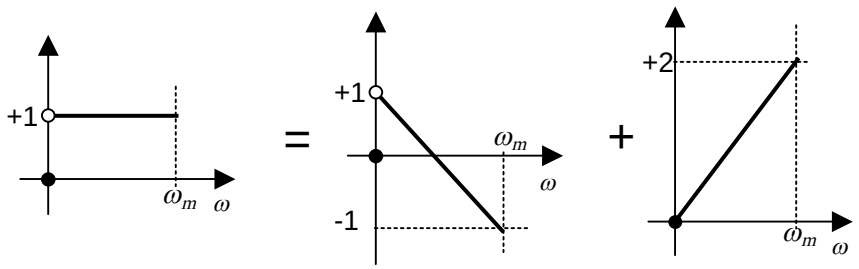

(a) Total imaginary part $Z'_I(\omega)$ (b) Regular components $Z'_{Ir}(\omega)$ (c) Singular components $Z'_{Is}(\omega)$

Figure 1 Modeling of imaginary part:

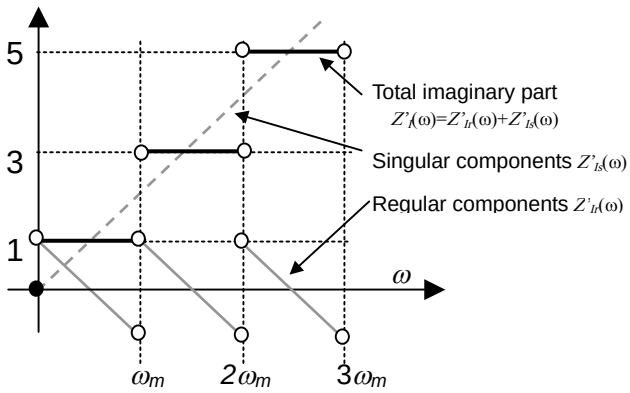

Figure 2 Behavior of imaginary part in high frequency area

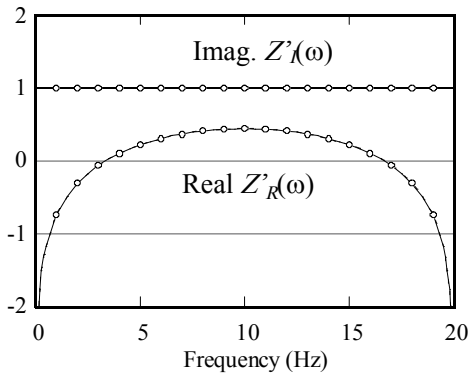

Figure 3 Calculated causal unit imaginary function $Z'(\omega)$

2.3 Calculation of Real Part

The causal real part $Z'_R(\omega)$ is calculated from the regular component $Z'_{Ir}(\omega)$ using the Hilbert transform in Eq.2.8. The value for $Z'_R(\omega)$ is obtained numerically as Cauchy's principal values of integral by setting the

focused frequency range at 0~20Hz ($\omega_m = 40\pi$). Figure 3 shows the computed real part $Z'_R(\omega)$ together with the imaginary part $Z'_I(\omega)$.
The calculated function $Z'_R(\omega)$ is smooth and symmetric about the center of the focused frequency range (10Hz in this case). Although the numerical integral is stable in general, the calculated function has logarithmic singularities in areas close to points of discontinuity (0Hz and 20Hz), so it is difficult to calculate the integral accurately in these areas.
However, it does not matter if the accuracy in these areas is low because the values in the areas are not used in the transform to the time domain in the next step. The circle marks in Figure 3 show the data points used in the transform. It is found that all of them are in the stable area.

$$Z'_R(\omega) = -\frac{1}{\pi}\int_{-\infty}^{\infty}\frac{Z_{Ir}(x)}{x-\varpi}dx \tag{2.8}$$

2.4 Calculation of Impulse Response

The author proposed some methods for the transform of the frequency dependent complex stiffness to the time domain (Nakamura, 2006a, 2006b). In the following, the transform of the causal unit imaginary function $Z'(\omega)$ obtained in the previous chapter to the time domain is carried out. Method B is utilized for the transform. If method C is used, the obtained impulse responses are all the same since the complex function is causal and nothing is modified.
The transform is conducted for the three models shown in Table 1. The name of each model implies the number of the time delay components. It can be thought that the larger the number, the higher the accuracy in the transform to the time domain.

Table 1. Transform data

Model Name	Number of Complex Data (N)	Frequency of Complex Data (Hz)	Time Step (sec)	Number of Time-delay Components (N-1)
3 terms	4	4., 8., 12., 16.	0.05	3
8 terms	9	2., 4., 6., 8., … 18.	0.05	8
18 terms	19	1., 2., 3., 4., … 19.	0.05	18

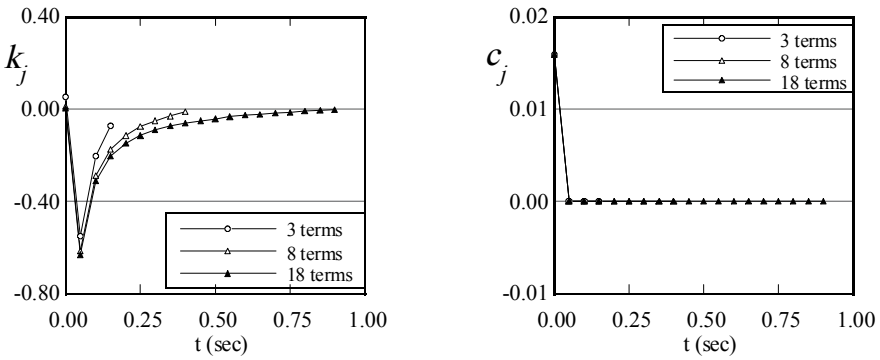

(a) Stiffness terms (k_j) (b) Damping terms (c_j)

Figure 4. Calculated impulse response

Figure 4 illustrates the impulse response obtained from the transform. The simultaneous components k_0 and m_0 are almost 0 except k_0 of the 3 term model. The reason is considered as the followings.
The real part of $Z'(\omega)$ is calculated by the Hilbert transform. Since the simultaneous components are not obtained from the Hilbert transform, the simultaneous components k_0 and m_0 , whish are related to the real part only, become 0. It is thought that the reason why k_0 of the 3 term model only is substantial is because the transform accuracy of this model is lowest.
As for the time delay components of the stiffness terms, the first term (k_1) is about -0.6 in any case. With an

increase in t, the impulse response value gradually increases toward 0. There is a tendency in which the smaller the number of terms for the time delay component, the more quickly the impulse response value approaches 0. With regard to the damping term, the same tendency is shown in all cases with the simultaneous component only. As for $Z'(\omega)$, the real part shows the symmetry at the center (10Hz) of the focused frequency range (0~20Hz) and the regular component of the imaginary part is skew-symmetric, so the time delay components $c_1 \sim c_{N-1}$ of the damping term must be 0 and $\Delta t\omega_m = 2\pi n$ where n=1,2,… In this case, Δt is set at 0.05sec as shown in table 2, so $\Delta t\omega_m$ becomes 2π.

From the above, the actual components of the impulse response of the causal unit imaginary function are the time delay component of the stiffness term (k_j where j=1,2,..) and the simultaneous component of the damping term (c_0). Then, $Z'(\omega)$ and the corresponding reaction $z'(t)$ can be indicated in Eqs. 2.9 and 2.10.

Figure 5 illustrates the complex stiffness recovered from all components of the impulse response by Eq. 2.9 together with the data points used for the transform (in the case of the model with 18 terms) of the causal unit imaginary function $Z'(\omega)$. Almost the same characteristics can be seen in all cases and correspond quite well to $Z'(\omega)$. The difference between each case occurs at the ends of the focused frequency range (near 0Hz and 20Hz in the figure). The proposed model can also be formulated using non-dimensional frequency and an upper limit of the focused frequency range can be arbitrarily varied.

$$Z'(\omega) = i\omega \cdot c_0 + \sum_{j=1}^{N-1} k_j \cdot e^{-i\omega t_j} \tag{2.9}$$

$$z'(t) = c_0 \cdot \dot{u}(t) + \sum_{j=1}^{N-1} k_j \cdot u(t - t_j) \tag{2.10}$$

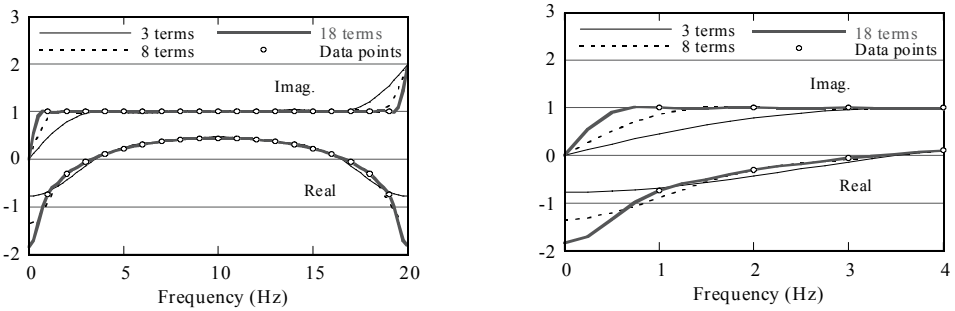

(a) Figure in 0~20Hz (b) Figure in 0~4Hz

Figure 5 Recovered complex stiffness

3. THE BIOT MODEL

As mentioned above, the Biot model has been regarded as one of the models which most closely approximate the hysteretic damping among causal models. A number of studies on the application of this model to time history response analyses have been carried out. In this paper, the characteristics of the proposed model are compared with those of the Biot model which is approximated using the Prony series by Makris and Zhang (2000).

Complex stiffness of the Biot model $S_b(\omega)$ is shown by Eq. 3.1 in the form corresponding to Eq. 2.4. K_0 and h indicate the static stiffness and damping ratio respectively. ε in Eq. 3.2 is an arbitrary real constant.

$$S_b(\omega) = K_0(1 + 2h \cdot Z_b(\omega)) \tag{3.1}$$

Where

$$Z_b(\omega) = \frac{2}{\pi}\left(\ln\sqrt{1 + \left(\frac{\omega}{\varepsilon}\right)^2} + i \cdot \tan^{-1}\left(\frac{\omega}{\varepsilon}\right) \right) \tag{3.2}$$

$Z_b(\omega)$ for the Biot model is considered as a function corresponding to the unit imaginary function shown in the previous chapter. In the following studies, the Biot model with ε =1.0 which relatively corresponds to the proposed model will be used. Eq. 3.1 in the time domain is led from Eq. 3.3. $z_b(t)$ indicates a reaction in the time domain corresponding to $Z_b(\omega)$ and it can be explained by Eq. 3.4 using the impulse response damping term $c_b(t)$.

$$F_b(t) = K_0 \cdot \left(u(t) + 2hz_b(t)\right) \tag{3.3}$$

Where

$$z_b(t) = \int_{-\infty}^{t} c_b(t-\tau) \cdot \dot{u}(\tau) d\tau \tag{3.4}$$

The solution of $c_b(t)$ can be given by Eq.3.5. γ indicates the Euler constant (0.5772).

$$c_b(t) = \frac{2}{\pi}\int_{-\infty}^{\varepsilon t} \frac{e^{-\xi}}{\xi} d\xi = -\frac{2}{\pi}\left(\ln|\varepsilon t| + \gamma + \sum_{n=1}^{\infty} \frac{(-1)^n (\varepsilon t)^n}{nn!}\right) \tag{3.5}$$

$c_b(t)$ in Eq. 3.5 was approximated by $c_{bp}(t)$ in Eq. 3.6 using the Prony series. The coefficients a_i and b_i are the coefficients for Prony series. They correspond to the coefficient g_i and $\varepsilon\lambda_i$ of N=4 in Makris and Zhang (2000), where $a_i = g_i / 0.36$ and $b_i = \varepsilon\lambda_i$

$$c_{bp}(t) = \sum_{i=1}^{4} a_i \cdot e^{\frac{-\varepsilon t}{b_i}} \tag{3.6}$$

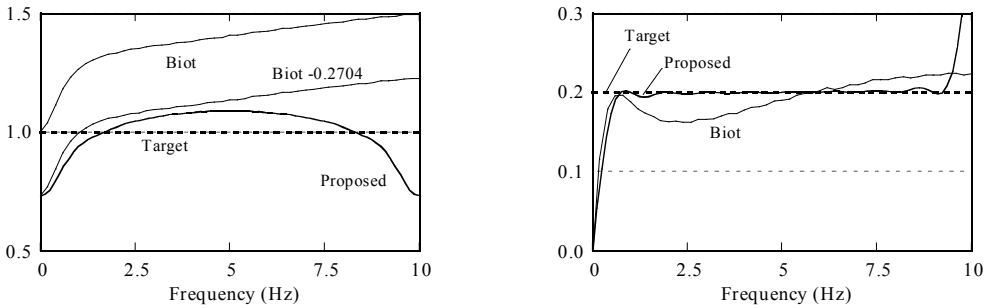

(a) Real parts / K_0, (b) Imaginary parts / K_0

Figure 6 Comparison of complex stiffness (h=10%) between the Biot model (Δt=0.01) and the proposed model (8 terms)

In Figure 6, $S'(\omega)$ of Eq. 2.5 calculated by the proposed model (8 terms) is compared with $S_b(\omega)$ of Eq. 3.1 calculated by the Biot model (Δt=0.01sec). The damping ratio h is set at 10%.

In the real part shown in Figure 6(a), the value of the proposed model is located between 0.73 and 1.09 corresponding to the target value 1.0. The value of the Biot model increases from 1.0 at 0Hz to 1.5 at 10Hz.

Using the constant (1.352), which makes the real part 0 at 0 Hz of the proposed model, the real part of the Biot model is modified for comparison by reducing a constant (0.2704 = 1.352 x 2h). The modified real part generally corresponds to that of the proposed model in the range from 0 Hz to 5Hz.

As for the imaginary part shown in Figure 6(b), the proposed model and the Biot model agree well to each other in the area of 0.6Hz or less. However, in the area greater than 0.6Hz, the Biot model differs from the target due to the fluttering while the proposed model almost agrees with the target except the vicinity of 10Hz.

4. TIME HISTORY RESPONSE ANALYSIS

A time history earthquake response analysis is carried out using the proposed causal hysteretic damping model in order to confirm its validity and effectiveness.

4.1 Equation of Motion

In the frequency domain, the equation of motion for earthquake response analyses with hysteretic damping can be written as Eq.4.1. $[M_S]$ and $[K_S]$ in this equation indicate the mass and stiffness matrix of a structure. $\{u(\omega)\}, y_0(\omega)$ and h are the structural displacement vector, input ground motion and damping ratio respectively. When applying $Z'(\omega)$ in place of the imaginary unit i, the equation of motion in the time domain can be expressed as Eq. 4.2 using $z'(t)$ in Eq.2.10.

$$(-\omega^2[M_S]+(1+2h\cdot i\cdot \mathrm{sgn}(\omega)[K_S])\{u(\omega)\}=\omega^2 y_0(\omega)[M_S]\{1\} \tag{4.1}$$

$$[M_S]\{\ddot{u}(t)\}+[K_S](\{u(t)\}+2h\{z'(t)\})=-\ddot{y}_0(t)[M_S]\{1\} \tag{4.2}$$

In cases where the damping ratio is not uniform in an entire structure, the element force $\{F_K(t)\}_E$ of Eq. 4.3 of each element can be calculated and superposed for all elements. The subscript E in Eq. 4.3 indicates the amount for the element.

$$\{F_K(t)\}_E=[K_S]_E(\{u(t)\}_E+2h_E\{z'(t)\}_E) \tag{4.3}$$

4.2 Time History Analysis of Layered Soil Model

In order to compare the proposed model with the Biot model, an earthquake response analysis of a layered soil model is performed.

The analysis model is shown in Figure 7. This analysis model has two layers on rigid rock. The shear wave velocity Vs of the upper layer is set at 100m/s and that of the lower layer is set at 200m/s. The damping ratio of the upper layer is set at 10% and that of the lower layer is 5%. A soil column model with a unit sectional area is used as an analysis model which is a one-dimensional 15 lumped mass system model with shear springs.

The analysis is carried out for the proposed model (8 term model, focused frequency range 0-10Hz) and the Biot model (ε =1.0, Δt=0.01sec) approximated using the Prony series. The analysis results are compared with the results of the frequency response analysis using the complex damping model. The input ground motion and conditions for the time history analysis and frequency analysis are the same as those for the 4 nodal model. The primary and the second eigenfrequencies of the model by the real eigenvalue analysis are 1.96Hz and 4.98Hz, respectively.

Figure 8 compares the time history waves (absolute acceleration, relative velocity and relative displacement) of the top node of the proposed model and the Biot model in the time range being 0~6 sec with the results obtained from the frequency response analysis. For each wave, the maximum value and the ratio to that of the frequency response analysis in the parenthesis are also described in the figure for comparison.

The time history waves for the proposed model almost agree to the results of the frequency response analysis as shown in Figure 8(a). However, with regard to the Biot model, a large difference is discernible in the phase between the time history wave and the frequency analysis result as shown in Figure 8(b).

It can be thought that this is so because the real value of the Biot model is about 1.3 times the target value (1.0) at the first eigen frequency (1.96Hz) of the model as shown in Figure 6 so the first eigen period of the Biot model becomes 10~15% shorter than that of the frequency analysis corresponding to the square root of 1.3.

Therefore, it can be said that the proposed model is more efficient than the Biot model because of the higher accuracy and the almost equal computational burden.

5. CONCLUSIONS

In this paper, an approximate causal hysteretic damping model was proposed. The model was made up using the

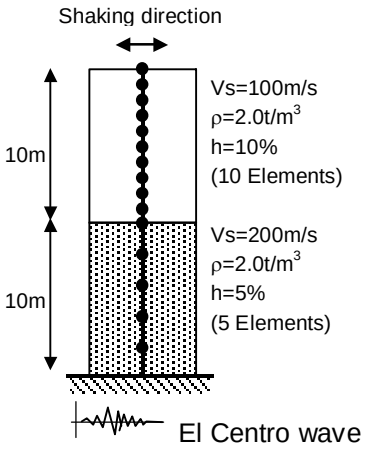

Figure 7 Layered soil model

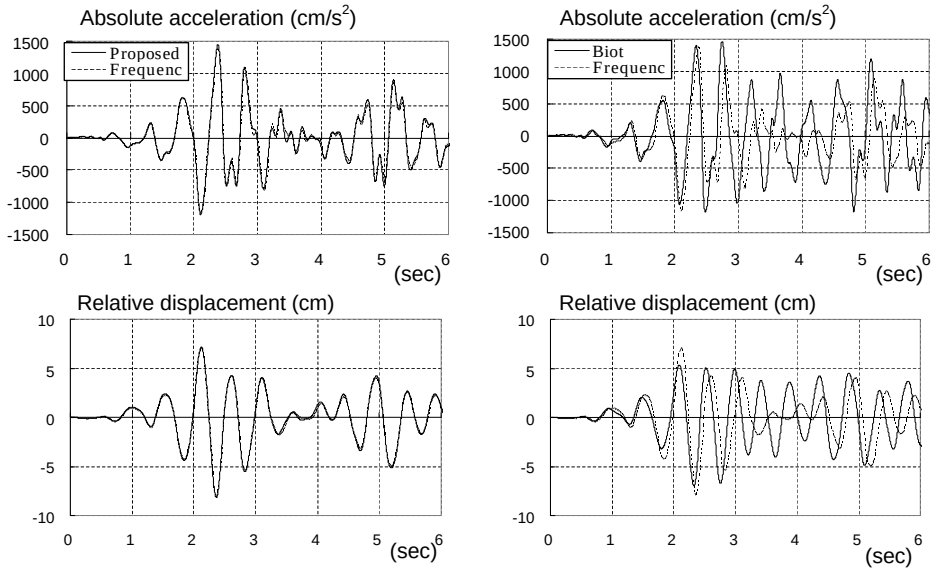

(a) Proposed model (8 terms) (b) The Biot model

Figure 8 Comparison of time history waves of top node

approximately causalized impulse response of the unit imaginary function that is a principle component of the ideal hysteretic damping. The impulse response was obtained by employing the method for transforming the complex stiffness to the time domain

First, the fundamental characteristics of this proposed model were studied. Then, the Biot model approximated using the Prony series was shown and the characteristics of the model were compared with those of the proposed model.

Moreover, earthquake response analyses of a layered soil model were carried out in order to compare the behavior of the proposed model with the Biot model. As a result, the applicability and the efficiency of the proposed model to time history response analyses corresponding to the Biot model were confirmed.

The details of this method are shown in Nakamura (2007).

REFERENCES

Chopra AK (2000). Dynamics of Structures - Theory and Applications to Earthquake Engineering 2nd Edition. *Prentice Hall*

Dobry R, Whitman RV, Rosset JM (1971). Soil Properties and the One-Dimensional Theory of Earthquake Amplification. *Research Report (Dept. of Civil Engineering MIT*;**R71-18**

Inaudi JA, Kelly JM (1995). Linear Hysteretic Damping and the Hilbert Transform, *Journal of Engineering Mechanics (ASCE)*; **121-5**:626-632

Makris N (1997). Causal Hysteretic Element. *Journal of Engineering Mechanics (ASCE)*; **123-11**:1209-1214

Biot MA (1958). Linear Thermodynamics and the Mechanics of Solids, *Proc. 3rd U .S. National Congress of Applied Mechanics (ASME)*; **6**: 1-18

Makris N, Zhang (2000). Time Domain Viscoelastic Analysis of Earth Structures. *Earthquake Engineering and Structural Dynamics*; **29**: 745-768

Nakamura N (2006a). A Practical Method to Transform Frequency Dependent Impedance to Time Domain. *Earthquake Engineering and Structural Dynamics*; **35**: 217-234

Nakamura N (2006b). .Improved Methods to Transform Frequency Dependent Complex Stiffnessto Time Domain. *Earthquake Engineering and Structural Dynamics* ; **35**: 1037-1050

Nakamura N (2007). A Practical Causal Hysteretic Damping. *Earthquake Engineering and Structural Dynamics* ; **36**: 597-617